CrossMark

# Knockdown of Cripto-1 inhibits the proliferation, migration, invasion, and angiogenesis in prostate carcinoma cells

Ding Wu[1], Zhan Shi[2], Hao Xu[1], Renfu Chen[1], Song Xue[1] and Xiaoqing Sun[1,*]

[1]*Department of Urology, The Affiliated Hospital of Xuzhou Medical University, Xuzhou, Jiangsu Province, People's Republic of China*

[2]*Shanghai Jiao Tong University School of Medicine, Shanghai, People's Republic of China*

*\*Corresponding author (Email, xqsunurology@163.com)*

Cripto-1 (CR-1) is a member of the epidermal growth factor-Cripto-1/FRL1/Cryptic gene family that plays a key role in the various malignant cancers. However, the role of CR-1 in prostate carcinoma (PCa) remains limited. The expression of CR-1 was down-regulated by small interfering RNA (siRNA). Western blot measured the expression levels of CR-1 and some related proteins. We performed Cell Counting Kit-8, 5-ethynyl-2-deoxyuridine (EdU) incorporation assay and flow cytometry to detect the cellular proliferation and cycle. The transwell assay was used to observe cellular migration and invasion. The ability of angiogenesis was evaluated by tube formation assay. Our results showed that CR-1 knockdown markedly inhibited cell proliferation and induced cycle arrest in G1 phase, as p21 and p27 were up-regulated, whereas cyclin D1 and cyclin E1 were diminished. Moreover, silencing of CR-1 dramatically inhibited cell migration and invasion, repressed matrix metalloproteinases, and disturbed epithelial-mesenchymal transition. CR-1 siRNA suppressed the secreted level of vascular endothelial growth factor, and reduced protein level of Vascular endothelial growth factor receptor 2. We further found that decreased CR-1 expression inhibited FAK/Src/PI3K and Wnt/β-catenin signalling in PCa cells. These results suggested CR-1 might be served as an effective therapeutic target in PCa.

**Keywords.** Angiogenesis; Cripto-1; Epithelial-mesenchymal transition; Metastasis; Proliferation; Prostate carcinoma

## 1. Introduction

Prostate carcinoma (PCa) is the most commonly diagnosed type of malignant cancer and is the third leading cause of death from cancer in males, with an affirmed 161,360 new cases and 26,730 deaths due to PCa reported in the US in 2017 (Siegel *et al.* 2017). The annual morbidity of PCa has shown sustained and stable growth, and has increased by 14% in the last 20 years (Das *et al.* 2016). Pharmacological and surgical androgen deprivation therapies are the primary modes of therapy for PCa, because most cases of early PCa begin as androgen-dependent cancers. Despite a series of efforts, the cancer will inevitably reoccur aggressively, with a considerable portion of victims succumbing to the disease. Eventually, the disease progresses to androgen-independent prostate carcinoma (AIPC), which is associated with a high mortality rate with limited available therapies. Therefore, there is an urgent need to search for efficient targets for the therapeutic intervention of PCa in order to improve patient survival.

Cripto-1 (CR-1, also referred to as TDGF-1) consists of several signal sequences for extracellular secretion, including a modified epidermal growth factor (EGF)-like domain,

conserved cysteine-rich domain, and short carboxy-terminus. CR-1 can function as a membrane-associated protein to promote signalling by certain proteins, including Nodal and GDF, while attenuating signalling by other ligands such as activins and transforming growth factor (TGF)-β. In addition, CR-1 may also modulate biological functions by activating the AKT and MAPK signalling pathways in direct cooperation with various transmembrane proteins such as GRP78, Glypican-1and Notch (Bianco *et al.* 2005b). A recent study (Lawrence *et al.* 2011) demonstrated that CR-1 is overexpressed in certain PCa cell lines; however, the functionality of CR-1 has yet to be ascertained.

EMT is a vital process for embryonic development, tissue remodeling, and tumorigenicity, and involves phenotypic changes including the loss of cell polarity, decreased cell adhesion ability, and the acquisition of metastatic capability (Nieto 2013). The down-regulation of epithelial (E)-cadherin is characterized as the hallmark of EMT, whereas the expression levels of mesenchymal markers are increased, such as neuronal (N)-cadherin, vimentin and fibronectin (FN) (Guan 2015). In several different types of tumors, EMT has been shown to be an important step promoting local infiltration and subsequent tumor metastasis through the

hematogenous lymphatics, with consequent lymphatic dissemination (Nieto 2013). There is also increasing evidence that EMT is regulated by the activation of various signalling pathways and is associated with different growth factors such as fibroblast growth factors (FGFs), TGF-β, and EGF (Thiery *et al.* 2009; Shi *et al.* 2016). MMPs belong to a family of zinc-dependent endopeptidases, whose main function is to degrade the extracellular matrix (ECM). Activation of MMPs is closely associated with the increased invasion, migration, and poor prognosis of several types of human cancers (Vaisanen *et al.* 2008). However, the role of CR-1 in the activation of MMPs in PCa remains unknown.

Angiogenesis involves endothelial cell proliferation, migration, and tubulogenesis. The new blood vessels formed can penetrate into the tumor tissue to provide alimentation and to remove metabolic waste; thus, angiogenesis is closely related to tumor growth and metastasis (Folkman 2004). VEGF has been characterized with regard to multiple effects relevant to the generation and preservation of tumor vasculature. These effects include induction of endothelial cell migration, and promotion of endothelial cell survival (Watanabe *et al.* 1997; Waldner and Neurath 2012). VEGFR2 is the major mitogenic mediator and permeability enhancing effects of VEGF (Corti and Simons 2017). Previous studies found the decreased VEGFR2 expression inhibits the angiogenesis of PCa (Saraswati *et al.* 2013). Rangel et al. (Rangel *et al.* 2012) detected CR-1, together with proangiogenic factors, during EMT in mammary epithelial cells, suggesting a potential role of CR-1 in angiogenesis. However, the role of CR-1 in the angiogenesis of PCa is not yet known.

Here, we employed human PCa cells to explore the relationship between CR-1 and cellular proliferation, migration, invasion, angiogenesis, and EMT processes in PCa, and to identify the possible signalling pathways mediating these effects.

## 2. Materials and methods

### 2.1 *Cell culture and antibodies*

Human PCa cell lines (PC3, DU145) were purchased from Chinese Academy of science (Shanghai, China). Human umbilical vascular endothelial cells (HUVECs) were obtained from Key-GEN biotech (Nanjing, China). PC3, DU145 and HUVEC cells were cultured in RPMI-1640 medium (HyClone, UT, USA) supplemented with 10% FBS at 37°C in a humidified incubator containing 5% $CO_2$. The following antibodies were used for Western blotting: rabbit anti-human CR-1, E-cadherin, N-cadherin, Vimentin, FN, total AKT, phosphorylated AKT (p-AKT), total GSK-3β, phosphorylated GSK3β (p-GSK3β), Src, phosphorylated Src (p-Src), p21, p27, β-catenin, β-actin were purchased from

Abcam, MA, USA; Rabbit anti-human MMP2, MMP9, total PI3K, phosphorylated PI3K (p-PI3K), total FAK, phosphorylated FAK (p-FAK), cyclin D1, cyclin E1 and VEGFR2 were purchased from Cell Signaling Technology, MA, USA; Mouse anti-human c-myc, β-catenin, PCNA were purchased from Santa Cruz Biotechnology, CA, USA. The horseradish peroxidase-conjugated goat anti-rabbit IgG and goat anti-mouse IgG secondary antibodies were purchased from Zhong Shan Biotechnology, Beijing, China.

### 2.2 *Small interfering RNA and transfection*

Inhibition of Cripto-1 expression in PCa cells was performed by CR-1 siRNA. Non–specific siRNA was used as negative controls. The negative control FAM (6-carboxy-fluorescein) siRNA was used to observe the transfection efficiency under fluorescence microscope. Both of these siRNA were designed, synthesized and purified by GenePharma (Shanghai, China), and stored at −20°C. The primers were listed as follow: CR-1 siRNA sense 5′-CAGCACA-GUAAGGAGCUAATT-3′ and antisense 5′-UUAGCUC-CUUACUGUGCUGTT-3′, the non-specific siRNA sense 5′-UUCUCCGAACGUGUCACGUTT-3′ and antisense 5′-ACGUGACACGUUCGGAGAATT-3′, negative control FAM siRNA sense 5′-UUCUCCGAACGUGUCACGUTT-3′ and antisense 5′-ACGUGACACGUUCGGAGAATT-3′. When cells were grown to 60 %, the siRNA was transfected using siLentFect Lipid Reagent (Bio-Rad, CA, USA) according to the manufacturer's instructions. 6 h later, the medium was changed to fresh RPMI-1640 with 10% FBS, and continued to culture for 48 h, cells were harvested for the following assays.

### 2.3 *RNA isolation and reverse transcription-quantitative-polymerase chain reaction (RT-qPCR)*

The total RNA was islotated by Trizol reagent according to the manufacturer's protocol. We use the spectrophotometer at 260 and 280 nm (A260/280) to measure the concentration of RNA in cells, then the extracted RNA was reverse-transcribed into cDNA using the PrimeScript RT-PCR kit (Takara, Tokyo, Japan) according to the manufacturer's recommendations. The reactions were performed in a total volume of 20 μL containing 3μg total RNA. RT-qPCR was performed on 7900HT Fast RT-PCR instrument (Applied Biosystems, Singapore) using SYBR-Green and the primers were listed as follows: 5′-AACCTGCTGCCTGAATGG-3′ (forward) and 5′-CAGACCCACAGTTCTCTTTGC-3′ (reverse) for CR-1; 5′-GCAAATTCCATGGCACCGT-3′ (forward) and 5′-TCGCCCCACTTGATTTTGG-3′ (reverse) for GAPDH. Primers were designed to produce an amplicon spanning at least 1 intron. Reactions were performed in a

total volume of 20 μL using 3 μL cDNA. The amplification procedure was performed as follows: 95°C for 30 s, followed by 40 cycles at 95°C for 5 s and 64°C for 34 s. Expression of Cripto-1 mRNA was assessed by evaluating CT values. The CT values of the Cripto-1 expression was normalized to GAPDH. The relative CR-1 expression level was explained as the relative quantification equation (RQ=$2^{-\Delta\Delta Ct}$). Meanwhile, the primer blasting and melting curve was ana-lyzed to ensure the specificity of amplification. Each sample was tested in triplicate.

## 2.4 Western blot analysis

For PCa cells, 48 h (RNAi) after transfection, cells were harvested from the plates. Then aliquots of cell extracts were separated on 10% SDS-polyacrylamide gels (Beyotime, Nantong, China), and were transferred to nitrocellulose membranes (NC, 0.22μm) at 0.2A for 2h. Membranes were blocked with 5% non-fat milk for 2 h, and incubated with primary antibodies at 4°C overnight. Membranes were washed and incubated with secondary antibody for 2 h. Membranes were then washed and scanned on the Odyssey Two-Color Infrared Imaging System (LI-COR Biotechnology, Lincoln, Nebraska, USA). The target bands intensities were normalized to β-actin for the relative expression.

## 2.5 Cell viability and proliferation analysis in vitro

Cell proliferation was assessed by Cell Counting Kit-8 (CCK-8, Beyotime, Nanjing, China). The WST-8 in CCK-8 solution, which was reduced by intracellular dehydrogenase into water-soluble orange yellow, can indirectly measure the number of viable cells. $5\times10^3$ cells were plated with 100 μL medium in 96-well cell plates and incubated overnight at 37°C. At different time points (24, 48, 72, and 96 h), the 10 μL CCK-8 reagents and 100 μL serem-free culture medium were added to each well instead. After incubation at 37°C for 2h, the absorbance value was measured at 450nm using the ELX-800 spectrometer reader (Bio-Tek Instrument, Winooski, USA). Each group has six independent samples. The EdU DNA Cell Proliferation Kit (Ruibo Biotech, Guangzhou, China) were used following the manufacturer's instructions. In brief, the cells, transfected with negative control or CR-1 siRNA for 24 h, $1\times10^4$ cells were cultured in 96-well plate at 37°C. After 24h, the 100 μM EdU were added to each well for 4 h at 37°C and fixed with 4 % paraformaldehyde. After permeabilization with 0.5 % Triton X-100, the cells were treated with 100 μL $1\times$ Apollo reaction cocktail for 30 min. Subsequently, cells were stained with DAPI for 30 min and washed with phosphatebuffered saline for 3 times, then visualized by fluorescence microscope.

## 2.6 Cell cycle assay

The PCa cells, treated with CR-1 siRNA or negative control siRNA after 48 h, were collected (centrifugation at 2000 rpm for 5 min) and washed with PBS, then fixed in 75% ethanol at 4°C for 18 h. Then, the cells were centrifuged and washed with PBS twice. At last, cells incubated with 100 μL RNase (Sigma, USA) at 37°C for 30 min, and stained with 400 μL PI each tube at 4°C for 30 min. The samples were measured at the wavelength of 488nm by flow cytometery (BD Biosciences, USA).

## 2.7 Cell migration assay

The cells were harvested at 24 h after transfection and seeded into the upper of the chambers with 8 μm pore size in 200 μL serum-free medium, then incubated in 24-well-plates with 600 μL 10% FBS supplemented medium for 18h. The non-migrated cells were removed by cotton swab, then fixed with 4% paraformaldehyde for 30 min and stained with 0.1% crystal violet at 37°C for 25 min, washed twice with PBS. The cells migrated through the chamber were observed by microscope ($\times200$ magnification).

## 2.8 Cell invasion assay

Each chamber was precoated with 50 μg Matrigel (BD Biosciences, NJ, USA) diluted by the serum-free medium at the ratio of 1:8, and the cells ($5\times10^4$) fixed with medium were seeded into the chamber's upper, the bottom chamber was filled with medium containing 10% FBS. The chambers were incubated for 36 h at 37°C in 5% $CO_2$ atmosphere. The rest steps were the same as the migration assay.

## 2.9 HUVECs growth assay

The HUVECs growth assay was tested by CCK-8. In brief, the HUVECs ($5\times10^3$) were suspended with 100 μL conditioned medium from non-specific control siRNA or CR-1 siRNA cells, and incubated at 37°C for 24 h in 96-well plates. The samples were examined with ELX-800 spectrometer reader (Bio-Tek Instrument, Winooski, USA) according to the manufacturer's instructions.

## 2.10 *Endothelial cell tube formation assay*

After transfection 24 h, the PCa cells ($1 \times 10^6$) were cultured in 6-well plate with serum-free medium for 24 h, and the medium was collected and centrifuged to eliminate the cell debris. The 48-well plate was precoated with 120 μL matrigel, and incubated at 37°C for 30 min. The HUVECs ($1 \times 10^4$) were suspended in 200 μL centrifuged medium and seeded into the 48-well plate at 37°C for 4 h. The number of capillary-like tubes was counted ($\times 100$) from the four randomly selected fields.

## 2.11 *ELISA for VEGF*

PC3 and DU145 cells were plated in 6-well plates at a density of $1 \times 10^6$ cells per well. Then, cells were transfected with siRNA with serum starvation. The supernatants were collected 24h after transfection. VEGF concentration was determined by Quantikine ELISA kits according to the manufacturer's instructions (Westang biotech, Shanghai, China).

## 2.12 *Statistical analysis*

All experiments were repeated 3 times and data were expressed as the mean ± standard deviation (SD). Statistical analysis was performed with SPSS 16.0 (Chicago, USA). The independent samples *t*-test was used to draw a comparison between two groups. $P < 0.05$ was considered to be statistically significant ($*P < 0.05$, $**P < 0.01$, $***P < 0.001$).

## 3. Results

### 3.1 *Efficiency of transfection of CR-1 siRNA*

To determine the transfection efficiency in PCa cells, we observed the intensity of green fluorescence under the fluorescence microscope, and found the efficiency of transfection of FAM siRNA was satisfactory which exceeded 70 % (figure 1A). The mRNA (figure 1B) and protein (figure 1C) expression levels of CR-1 were
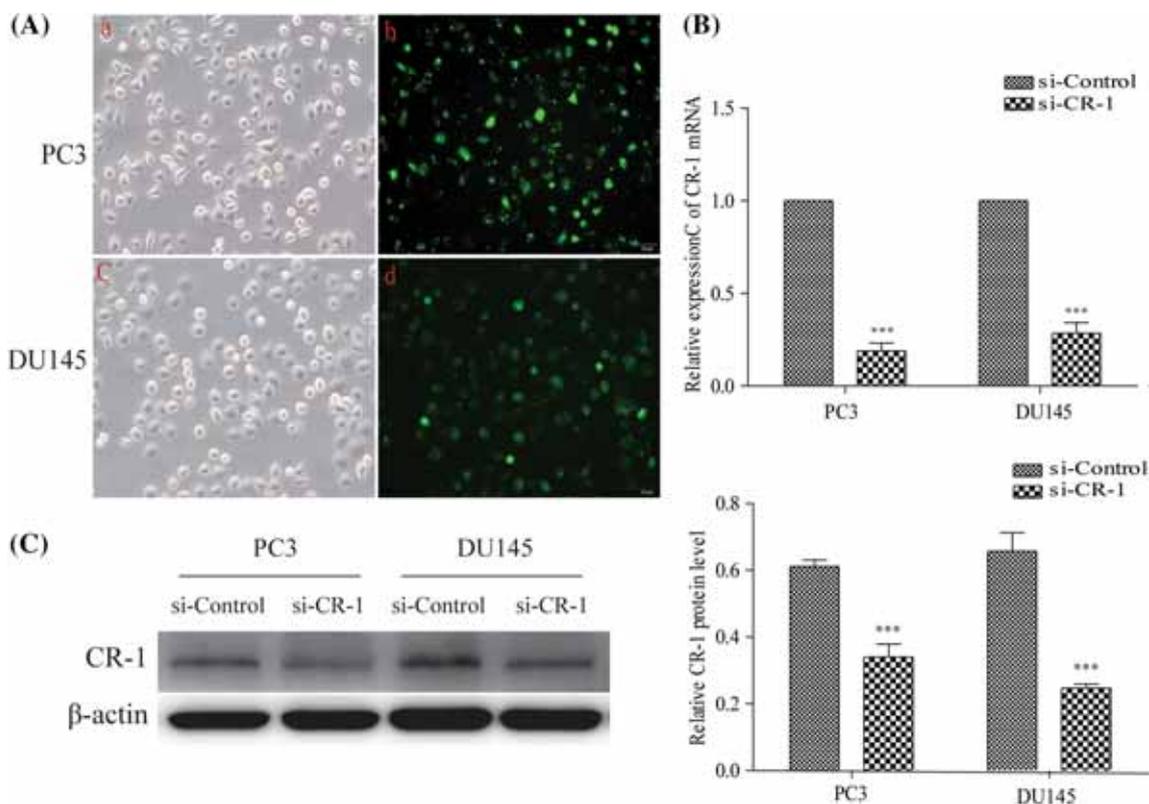


**Figure 1.** Effects of CR-1 siRNA on CR-1 expression of PC3 and DU145. (**A**) The fluorescent microscopy image assay was used to observe the transient transfection efficiency. The two pictures on the *left* (*a* and *c*) are optical micrographs and the *right* pictures (*b* and *d*) are the fluorescence micrographs. Intensity of green fluorescence showed the transfection efficiency. (**B**) mRNA and (**C**) protein expression levels of Cripto-1 were detected in PC3 and DU145 transfected with Cripto-1 siRNA or non-specific siRNA by RT-qPCR and western blot, respectively. The relative density of CR-1 protein is expressed as the ratio (CR-1/β-actin). Data represent the mean ± SD of three independent experiments. ($***P < 0.001$.)
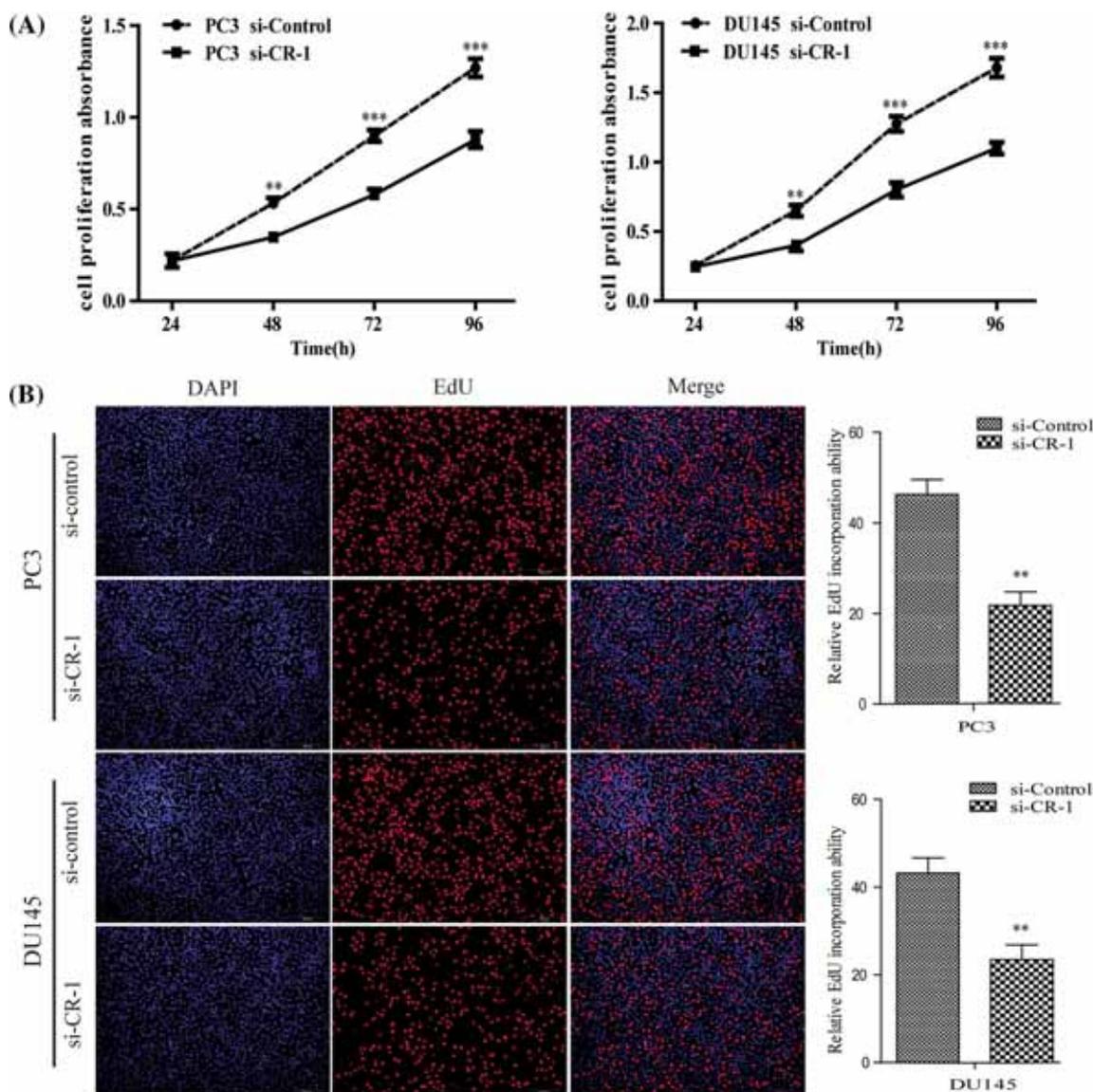
**Figure 2.** Silencing of CR-1 blocks cell proliferation and arrests cycle in PCa cells. The proliferative abilities of CR-1 siRNA transfected cells were assessed by CCK-8 assay and EdU incorporation assay. The PCa cell growth was measured by CCK-8 assay at the indicated time (**A**). (**B**) Representative EdU analysis of cell proliferation. DAPI (*blue*) was used to stain nucleus and EdU (*red*) showed the incorporated cells; Quantitative analysis of the relative cell proliferation rate. The value of CR-1 knockdown cells was normalized to that of control group. (**C**) Representative images showed knockdown of CR-1 with siRNA arrested the cell cycle in the G1 phase. (**D**) The cycle-associated protein levels of cyclins and Cip/Kip families, such as cyclin D1, cyclin E1, p21, and p27 were tested by western blot. All data represent the means $\pm$ SD of triplicates. (*$P<0.05$, **$P<0.01$, ***$P<0.001$.)

suppressed after transfection with CR-1 siRNA in both PC3 and DU145 cells.

### 3.2 *Down-regulation of CR-1 inhibits cellular proliferation and induces cellular cycle arrest*

To investigate the role of down-regulation of CR-1 on proliferation, we performed CCK-8 assay and observed cellular

proliferation was decreased (figure 2A). Afterwards, we used the EdU incorporation assay to examine the effects of CR-1 on cell proliferation, and found the number of PCa cells incorporating EdU was decreased after CR-1 knockdown (figure 2B). To better understand whether the reduced proliferation was associated with the cell cycle arrest, we carried out the flow cytometry; the results showed that CR-1 knockdown cells were arrested in the G1 phase (figure 2C). Western blot showed that CR-1 knockdown decreased the
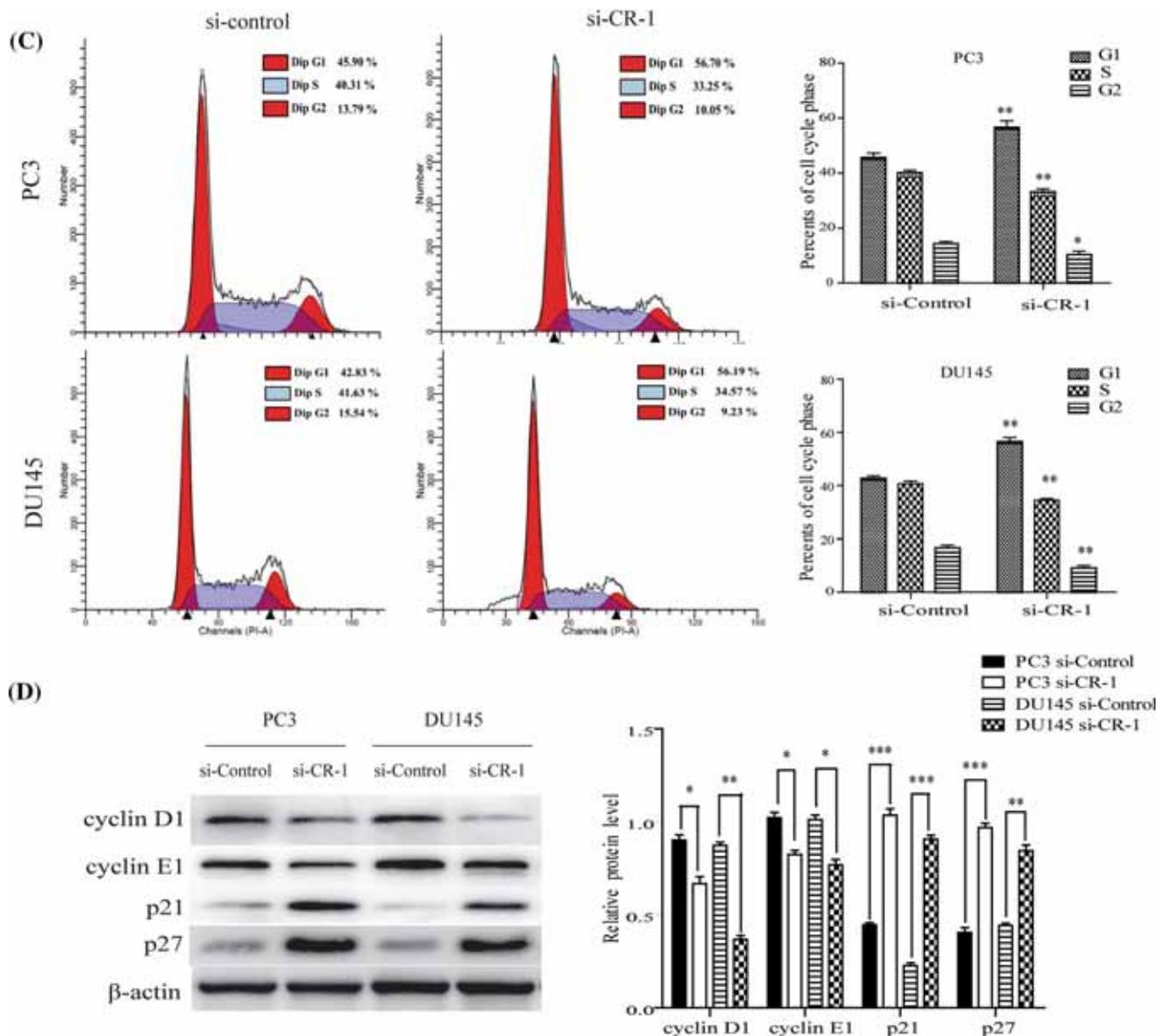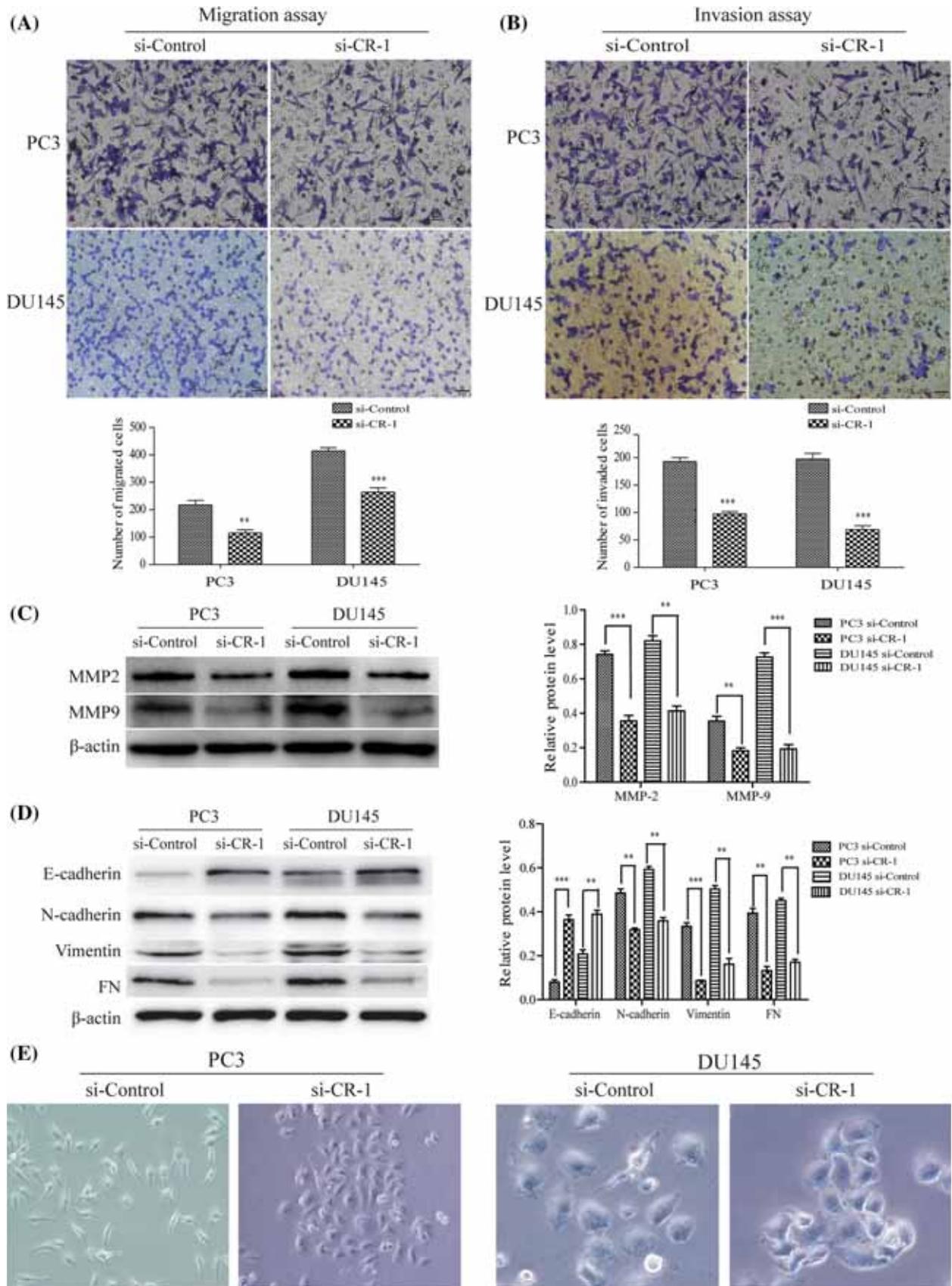
**Figure 2.** continued

cyclin D1 and cyclin E1, whereas increased p21 and p27 (figure 2D).

### 3.3 *Down-regulation of CR-1 inhibits the activities of migration and invasion*

To address whether CR-1 siRNA had an effect on cellular mobility and invasion, the transwell assay was carried out. After transfection with CR-1 siRNA, the activities of cell migration (figure 3A) and invasion (figure 3B) were weaker than that of control. These results suggested that CR-1

**Figure 3.** Silencing of CR-1 blocks PCa cells migration and ▶ invasion. The abilities of migration (**A**) and invasion (**B**) were tested by transwell chambers. Representative images showing the cells in CR-1 siRNA groups were significantly decreased compared to the control groups. (**C**) The protein levels of MMP-2 and MMP-9 in PC3 and DU145 cells were determined by Western blot. (**D**) Western blot was also performed to examine the protein levels of E-cadherin, N-cadherin, Vimentin, and FN. (**E**) Changes in cell morphology between negative control siRNA and CR-1 siRNA group cells. The values represent the means ± SD of three experiments performed in triplicate. (**P<0.01, ***P<0.001.)

**(A)**

Migration assay

si-Control    si-CR-1

PC3

DU145



**(B)**

Invasion assay

si-Control    si-CR-1

PC3

DU145



**(C)**

PC3    DU145

si-Control    si-CR-1    si-Control    si-CR-1

MMP2

MMP9

β-actin



**(D)**

PC3    DU145

si-Control    si-CR-1    si-Control    si-CR-1

E-cadherin

N-cadherin

Vimentin

FN

β-actin



**(E)**

PC3

si-Control    si-CR-1

DU145

si-Control    si-CR-1

knockdown in PCa cells inhibited the cellular migration and invasion.

## 3.4 *Down-regulation of CR-1 inhibits the expression of MMP-2 and MMP-9*

It has been demonstrated that MMPs was closely related to invasion and migration. We performed the western blot to detect the expression of MMPs as compared to the control group. The results demonstrated that the knockdown of CR-1 weakened remarkably the protein levels of MMP-2 and MMP-9 in PCa cells (figure 3C).

## 3.5 *Down-regulation of CR-1 inhibits the EMT*

EMT is a crucial step in promoting tumorigenesis, and so we detect the effects of CR-1 knockdown on EMT by Western blot. The results showed that after transfection with CR-1 siRNA, the biomarker of epithelial: E-cadherin was over-expressed, while the mesenchymal markers such as N-cadherin, vimentin and FN were reduced dramatically (figure 3D), as well as the morphological change occurred (figure 3E). The PC3 lost its spindle-shaped motile and the DU145 exhibited an increased ability of cell-cell adherence, as compared to control cells. These results suggested that CR-1 was involved in the progression of PCa through the regulation of EMT.

## 3.6 *Down-regulation of CR-1 inhibits angiogenesis in vitro*

To evaluate the role of CR-1 in angiogenesis of PCa, we performed angiogenesis assay. The condition medium containing secreted cytokines was collected from non-specific or CR-1 knockdown PCa cells, and served as the tube formation and the growth of HUVECs assays. The average number of complete tube-like structures formed by HUVECs in conditioned medium from CR-1 knockdown in PCa cells was decreased dramatically (figure 4A). Besides, in the HUVECs growth assay, the conditioned medium with CR-1 knockdown from PC3 and DU145 substantially inhibited cell proliferation (figure 4B). Here we investigated whether the role of CR-1 on angiogenesis was mediated by regulating VEGF secretion and VEGFR2 expression. We observed if VEGF secretion level was regulated by CR-1 in PCa cells using ELISA test. As shown in figure 4C, VEGF secretion level was negatively regulated by CR-1 siRNA in both PC3 and DU145 cells, respectively. Moreover, western blot showed the VEGFR2 protein level was dramatically reduced after being transfected with CR-1 siRNA. Our data showed no significant

change in the expression of ERK and p-ERK after transfection with CR-1 siRNA (figure 4D). The data implied that the inhibition of tube formation of HUVECs might be related to other signalling pathways (not preclude the p38 and JNK signalling ways) (Kim *et al.* 2013). The specific mechanism should be further explored.

## 3.7 *Down-regulation of CR-1 inhibits the FAK/Src/ PI3K and Wnt/β-catenin signalling pathways*

Numerous reports have supported that FAK/Src/PI3K pathway plays a key regulatory role during tumorigenesis. Accordingly, we investigate the proteins of FAK, Src, PI3K, AKT, GSK-3β and their phosphorylated proteins which were key proteins in signalling pathway. We found phosphorylated proteins (figure 5A) were markedly decreased in PCa cells with CR-1 knockdown, while the total proteins showed no significant change compared to control group. In addition, many reports have demonstrated that Wnt/β-catenin pathway also plays a key role in neoplastic development, and was associated with EMT. So, we performed western blot to detect the pathway related proteins, including c-myc, PCNA and β-catenin, and these proteins were obviously decreased in both two PCa cells transfected with CR-1 siRNA (figure 5B). These results suggested that silencing of CR-1 inhibited the FAK/Src/PI3K and Wnt/β-catenin signalling pathways in PCa cells.

## 4.  Discussion

CR-1 is a multifunctional embryonic protein that is overexpressed in several embryonic tissues and malignant tumors, but rarely in normal adult tissues (Nagaoka *et al.* 2013). The carcinogenic properties of CR-1, including the promotion of cell differentiation, tumorigenesis and EMT, have been demonstrated in various cancers (Klauzinska *et al.* 2014), although knowledge of the biological roles of CR-1 in PCa remains limited. In this study, we found that silencing CR-1 expression suppressed the proliferation, migration, invasion, angiogenesis, and EMT in PCa cells, and further inhibited the expression of related proteins including those involved in the FAK/Src/PI3K and Wnt/β-catenin signalling pathways. Our results suggest that CR-1 might play an important role in the development and aggressive behavior of PCa.

   Previous studies have shown that up-regulated CR-1 can stimulate cellular proliferation in different cancers (Sun *et al.* 2016, Yoon *et al.* 2011); therefore, we supposed that CR-1 may also have an effect on the proliferation of PC3 and DU145 cells. In support of this, the CCK-8 and EDU assays showed that silencing CR-1 decreased the proliferation both of PC3 and DU145 cells. In addition, flow cytometry showed that knockdown of CR-1 with siRNA arrested the
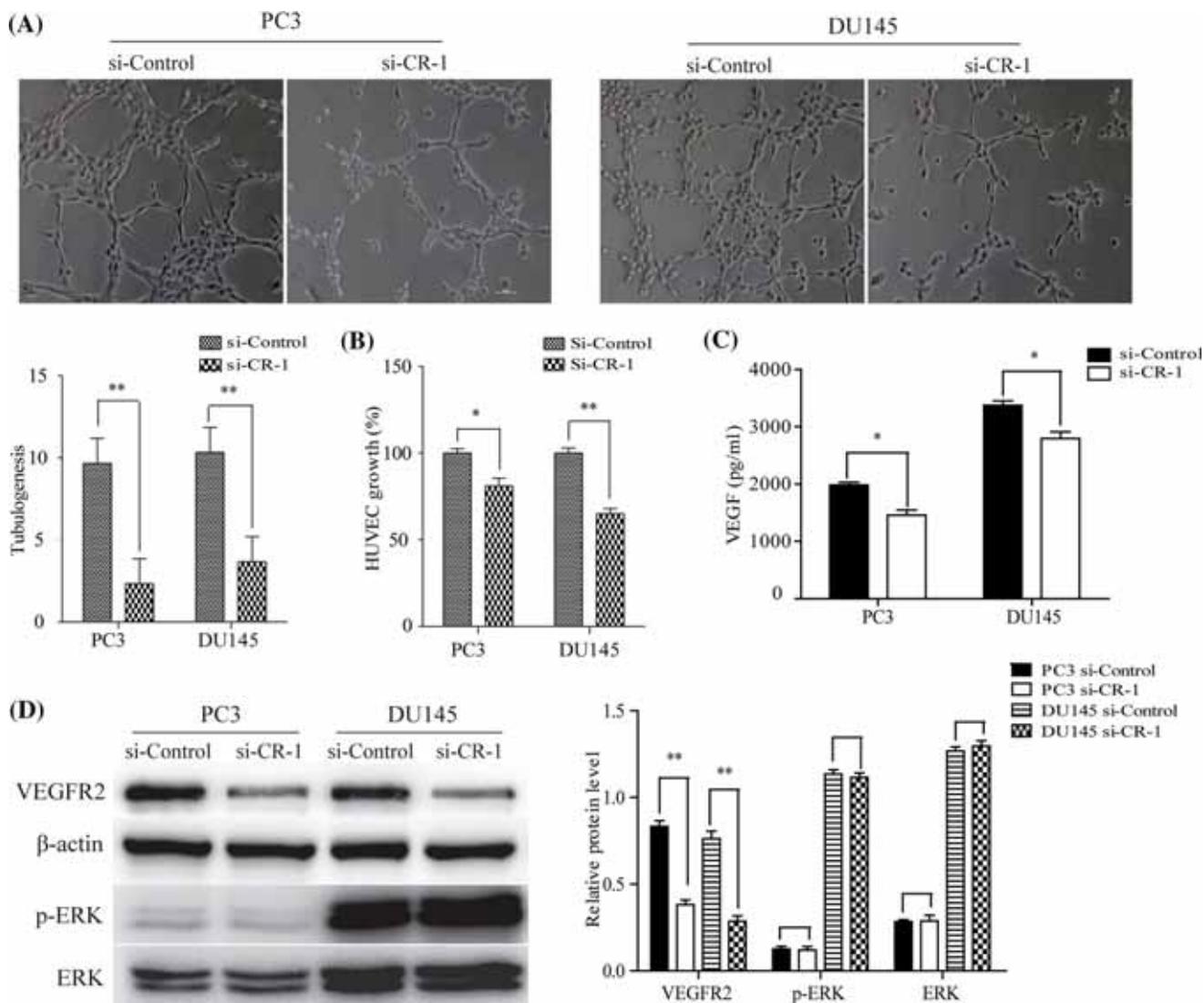
**Figure 4.** Silencing of CR-1 negatively regulates angiogenesis in PC3 and DU145. (**A**) Representative images were taken in *situ* for tube formation in the supernatant of PC3 and DU145 (×100). The ability of tube formation was evaluated by the number of tube. The average number of entire tubular structures formed by HUVECs from CR-1 knockdown in PC3 or DU145 was decreased compared with control. (**B**) HUVEC growth assay was used to detect the HUVECs proliferation. CR-1 siRNA negatively regulated the proliferation of HUVECs. (**C**) The secreted level of VEGF was determined by ELISA assay. VEGF secretion level was significantly inhibited by CR-1 siRNA in both PC3 and DU145 cells, respectively. (**D**) Representative analysis of the relative protein levels of VEGFR2, p-ERK and ERK in CR-1 knockdown and control group. Data were shown as mean ± SD for triplicate determinations. (*$P<0.05$, **$P<0.01$.)

cell cycle in the G1 phase. In general, cell cycle regulation depends on many elements that strictly regulate the transduction and duplication of genetic information, including cyclins, cyclin-dependent kinases (CDKs), and cyclin-dependent kinase inhibitors (CDKIs). The G1 transition is mainly modulated by the cyclin E–CDK2 and cyclin D1–CDK4 complexes. Cyclin–CDK complexes are precisely regulated by Cip1/Kip1 proteins such as p21 and p27, which can bind to and consequently weaken the activity of CDKs at the G1/S cell-cycle checkpoint (Eigeliene *et al.* 2008). Our results demonstrated that CR-1 knockdown increased the expression levels of both p21 and p27, which might subsequently inhibit the expression of cyclin E1 and cyclin D1, and eventually induce the observed cell cycle arrest in the G1 phase.

Metastasis is the major factor that negatively affects the prognosis of patients with cancer and is the cause of most cancer-related deaths. Tumor metastasis is a complex multistep process comprising cell adhesion, motility, degradation of the ECM, angiogenesis, and migration (Weng and Yen 2010). Consequently, disruption of one or more of these above steps in cancer development may suggest an
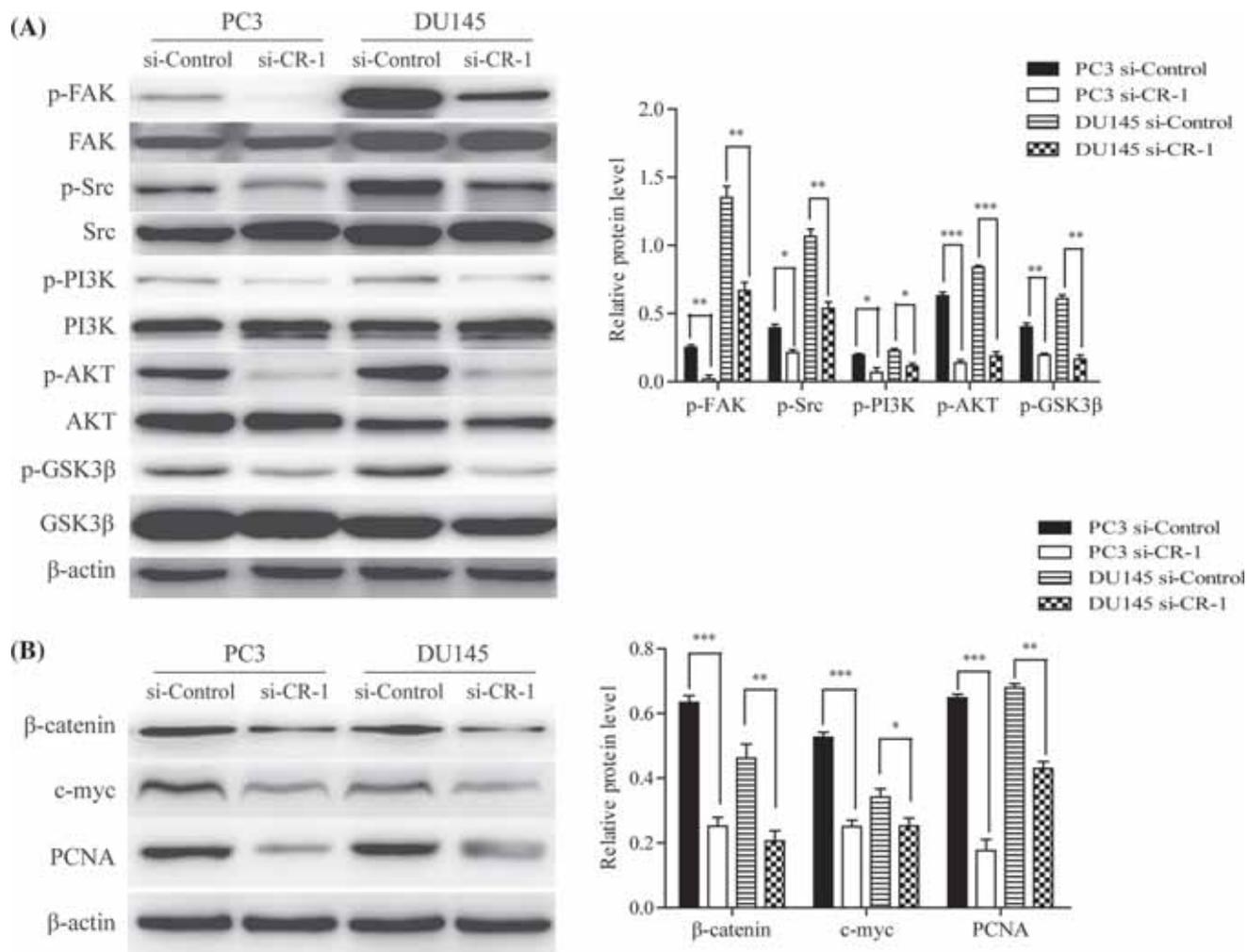
**Figure 5.** Silencing of CR-1 affects the related signalling molecules in PCa cells. (**A**) Western blot showed the changes in FAK, Src, PI3K, AKT, GSK-3β and their phosphorylated proteins after transfected with CR-1 siRNA. (**B**) Western blotting was used to demonstrate the effect of CR-1 suppression on Wnt/β-catenin pathway. β-actin was used as a loading control. Data were shown as mean ± SD. (*$P<0.05$, **$P<0.01$, *** $P<0.001$.)

underlying strategy for anti-carcinoma treatment (Nam and Shon 2009). Previous work has suggested that CR-1 can stimulate cell migration, invasion, EMT, and angiogenesis (Bianco *et al.* 2005a, Normanno *et al.* 2004) in human cancer cells; nevertheless, information of the biological effects of CR-1 in PCa remains limited. In this study, we observed that down-regulation of CR-1 increased level of the the epithelial cell biomarker E-cadherin, and correspondingly, the expression levels of the mesenchymal cell biomarkers such as N-cadherin, vimentin and FN were reduced in PC3 and DU145 cells. Moreover, knockdown of CR-1 expression with siRNA changed the morphology of PC3 cells from the fibroblast-like spindle shape to an egg-like or polygon, and enhanced the aggregation of DU145 cells. These results suggest a potentially important role of CR-1 during EMT in PCa, which is consistent with a recent

study (Liu et al. 2017). MMP-2 and MMP-9, which belong to the family of gelatinases, are particularly important molecules in the progression of cancer. We found that silencing CR-1 attenuated the invasiveness of PCa cells, which might be due to the accompanying decreased expression levels of MMP-2 and MMP-9. In addition, CR-1 siRNA transfection resulted in weakened angiogenic activity through the reduction of tube formation and endothelial cell proliferation in HUVECs. Several studies have reported that VEGR2 can mediate activation of the MAPK (p38, ERK, and JNK) and FAK signalling pathways. In general, this VEGFR2-mediated signal transduction is mainly implemented by the activation of extracellular signal-regulated kinase (ERK) in endothelial cells (Becker *et al.* 2001). However, our data showed no significant change in the expression of ERK and p-ERK in PC3 and DU145 cells after

transfection with CR-1 siRNA. These results appear to be inconsistent with previous research (Terry *et al.* 2015) which may be related to the use of different PCa cell lines. Therefore, the specific mechanisms need to be further verified.

There is accumulating evidence that many molecular and microenvironmental factors can promote EMT in different types of tumor cells, including FAK and Wnt (Sabbah *et al.* 2008). FAK, a cytoplasmic kinase, is involved in the cadherin-mediated adhesions of epithelial cells during the EMT. In general, the accumulation of FAK results in its autophosphorylation and ensures that it binds to the SH2 domain of Src. Conversely, Src can also phosphorylate FAK at multiple amino acid residues to strengthen the activity of FAK (El-Haibi *et al.* 2012). The activated FAK/Src complex can successively phosphorylate PI3K and AKT, resulting in disordered activation of several essential biological processes, including increased cell proliferation, migration, and angiogenesis (Manning and Cantley 2007). Glycogen synthase kinase 3β (GSK-3β) generally acts as a downstream signalling protein molecule of AKT (Ackermann *et al.* 2010). Once it is inactivated by phosphorylation, reducing its degradation, β-catenin largely accumulates in the cytoplasm and enters the nucleus to eventually form a complex that modifies the biological activity. Moreover, previous study suggested that growth inhibition by GSK-3β inactivation was associated with an increase in the levels of cyclin-dependent kinase inhibitors such as p21and p27 (Guo *et al.* 2017). β-catenin is also considered to be a key regulator of the Wnt pathway, and PCNA and c-myc were identified as putative downstream targets of the Wnt/β-catenin signalling pathway (Kuhl and Kuhl 2013). Consequently, we performed western blot analysis to detect the expression of proteins related to FAK/Src/PI3K and Wnt/β-catenin signalling pathways, which showed that silencing of CR-1 can not only decrease the expression levels of β-catenin, PCNA and c-myc, but also reduce the expression of p-FAK, p-Src, p-PI3K, p-Akt, and p-GSK-3β. In our future work, we will concentrate on gaining a more accurate understanding of the mechanism by which CR-1 affects the activation of these two signalling pathways by using suitable inhibitors, and explore whether these two signalling pathways might work together in the development and progression of PCa.

Taken together, our results demonstrate that silencing of CR-1 inhibits the proliferation of PCa cells by blocking the cell cycle in the G1 phase, and attenuates the cells' angiogenesis capability. Moreover, our results suggest that the migration and invasion abilities of PCa cells might be reduced by suppressing the MMPs and EMT, as well as by inhibiting the FAK/Src/PI3K and Wnt/β-catenin signalling pathways. Thus, targeting CR-1 might be a useful biological therapy for PCa.

## References

Ackermann TF, Kempe DS, Lang F and Lang UE 2010 Hyperactivity and enhanced curiosity of mice expressing PKB/SGK-resistant glycogen synthase kinase-3 (GSK-3). *Cell. Physiol. Biochem.* **25** 775−786

Becker PM, Verin AD, Booth MA, Liu F, Birukova A and Garcia JG 2001 Differential regulation of diverse physiological responses to VEGF in pulmonary endothelial cells. *Am. J. Physiol. Lung. Cell. Mol. Physiol.* **281** L1500−L1511

Bianco C, Strizzi L, Ebert A, Chang C, Rehman A, Normanno N, Guedez L, Salloum R, Ginsburg E, Sun Y, *et al.* 2005a Role of human cripto-1 in tumor angiogenesis. *J. Natl. Cancer Inst.* **97** 132−141

Bianco C, Strizzi L, Normanno N, Khan N and Salomon DS 2005b Cripto-1: an oncofetal gene with many faces. *Curr. Top. Dev. Biol.* **67** 85−133

Corti F and Simons M 2017 Modulation of VEGF receptor 2 signaling by protein phosphatases. *Pharmacol. Res.* **115** 107−123

Das DK, Osborne JR, Lin HY, Park JY and Ogunwobi OO 2016 miR-1207-3p Is a novel prognostic biomarker of prostate cancer. *Transl. Oncol.* **9** 236−241

Eigeliene N, Harkonen P and Erkkola R 2008 Effects of estradiol and medroxyprogesterone acetate on expression of the cell cycle proteins cyclin D1, p21 and p27 in cultured human breast tissues. *Cell Cycle*. **7** 71−80

El-Haibi CP, Singh R, Gupta P, Sharma PK, Greenleaf KN, Singh S and Lillard JW Jr. 2012 Antibody microarray analysis of signaling networks regulated by Cxcl13 and Cxcr5 in prostate cancer. *J. Proteomics Bioinform.* **5** 177−184

Folkman J 2004 Endogenous angiogenesis inhibitors. *APMIS*. **112** 496−507

Guan X 2015 Cancer metastases: challenges and opportunities. *Acta. Pharm. Sin. B.* **5** 402−418

Guo H, Luo H, Yuan H, Xia Y, Shu P, Huang X, Lu Y, Liu X, Keller ET, Sun D *et al.* 2017 Litchi seed extracts diminish prostate cancer progression via induction of apoptosis and attenuation of EMT through Akt/GSK-3beta signaling. *Sci. Rep.* **7** 41656

Kim GD, Cheong OJ, Bae SY, Shin J and Lee SK 2013 6"-Debromohamacanthin A, a bis (indole) alkaloid, inhibits angiogenesis by targeting the VEGFR2-mediated PI3K/AKT/mTOR signaling pathways. *Mar. Drugs.* **11** 1087−1103

Klauzinska M, Castro NP, Rangel MC, Spike BT, Gray PC, Bertolette D, Cuttitta F and Salomon D. 2014 The multifaceted role of the embryonic gene Cripto-1 in cancer, stem cells and epithelial-mesenchymal transition. *Semin. Cancer Biol.* **29** 51−58

Kuhl SJ and Kuhl M 2013 On the role of Wnt/beta-catenin signaling in stem cells. *Biochim. Biophys. Acta.* **1830** 2297−2306

Lawrence MG, Margaryan NV, Loessner D, Collins A., Kerr KM, Turner M, Seftor EA, Stephens CR, Lai J, Postovit LM *et al.* 2011 Reactivation of embryonic nodal signaling is associated with tumor progression and promotes the growth of prostate cancer cells. *Prostate.* **71** 1198−1209

Liu Y, Qin Z, Yang K, Liu R and Xu Y 2017 Cripto-1 promotes epithelial-mesenchymal transition in prostate cancer via Wnt/beta-catenin signaling. *Oncol. Rep.* **37** 1521−1528

Manning BD and Cantley LC 2007 AKT/PKB signaling: navigating downstream. *Cell.* **129** 1261−1274

Nagaoka T, Karasawa H, Turbyville T, Rangel MC, Castro NP, Gonzales M, Baker A, Seno M, Lockett S, Greer YE *et al.* 2013 Cripto-1 enhances the canonical Wnt/beta-catenin signaling pathway by binding to LRP5 and LRP6 co-receptors. *Cell. Signal.* **25** 178−189

Nam KS and Shon YH 2009 Suppression of metastasis of human breast cancer cells by chitosan oligosaccharides. *J. Microbiol. Biotechnol.* **19** 629−633

Nieto MA 2013 Epithelial plasticity: a common theme in embryonic and cancer cells. *Science.* **342** 1234850

Normanno N, De Luca A, Bianco C, Maiello MR, Carriero MV, Rehman A, Wechselberger C, Arra C, Strizzi L, Sanicola M *et al.* 2004 Cripto-1 overexpression leads to enhanced invasiveness and resistance to anoikis in human MCF-7 breast cancer cells. *J. Cell. Physiol.* **198** 31−39

Rangel MC, Karasawa H, Castro NP, Nagaoka T, Salomon DS and Bianco C 2012 Role of Cripto-1 during epithelial-to-mesenchymal transition in development and cancer. *Am. J. Pathol.* **180** 2188−2200

Sabbah M, Emami S, Redeuilh G, Julien S, Prevost G, Zimber A, Ouelaa R, Bracke M, De Wever O and Gespach C 2008 Molecular signature and therapeutic perspective of the epithelial-to-mesenchymal transitions in epithelial cancers. *Drug Resist. Updat.* **11** 123−151

Saraswati S, Kumar S and Alhaider AA 2013 alpha-santalol inhibits the angiogenesis and growth of human prostate tumor growth by targeting vascular endothelial growth factor receptor 2-mediated AKT/mTOR/P70S6K signaling pathway. *Mol. Cancer.* **12** 147

Shi Z, Wu D, Tang R, Li X, Chen R, Xue S, Zhang C and Sun X 2016 Silencing of HMGA2 promotes apoptosis and inhibits migration and invasion of prostate cancer cells. *J. Biosci.* **41** 229−236

Siegel RL, Miller KD and Jemal A 2017 Cancer statistics 2017. *CA Cancer J. Clin.* **67** 7−30

Sun G, Yan SS, Shi L, Wan ZQ, Jiang N, Fu LS, Li M and Guo J 2016 MicroRNA-15b suppresses the growth and invasion of glioma cells through targeted inhibition of cripto-1 expression. *Mol. Med. Rep.* **13** 4897−4903

Terry S, El-Sayed IY, Destouches D, Maille P, Nicolaiew N, Ploussard G, Semprez F, Pimpie C, Beltran H, Londono-Vallejo A *et al.* 2015 CRIPTO overexpression promotes mesenchymal differentiation in prostate carcinoma cells through parallel regulation of AKT and FGFR activities. *Oncotarget.* **6** 11994−12008

Thiery JP, Acloque H, Huang RY and Nieto MA 2009 Epithelial-mesenchymal transitions in development and disease. *Cell.* **139** 871−890

Vaisanen AH, Kallioinen M and Turpeenniemi-Hujanen T 2008 Comparison of the prognostic value of matrix metalloproteinases 2 and 9 in cutaneous melanoma. *Hum. Pathol.* **39** 377−385

Waldner MJ and Neurath MF 2012 Targeting the VEGF signaling pathway in cancer therapy. *Expert Opin. Ther. Targets.* **16** 5−13

Watanabe Y, Lee SW, Detmar M, Ajioka I and Dvorak HF 1997 Vascular permeability factor/vascular endothelial growth factor (VPF/VEGF) delays and induces escape from senescence in human dermal microvascular endothelial cells. *Oncogene.* **14** 2025−2032

Weng CJ and Yen GC 2010 The in vitro and in vivo experimental evidences disclose the chemopreventive effects of Ganoderma lucidum on cancer invasion and metastasis. *Clin. Exp. Metastasis.* **27** 361−369

Yoon HJ, Hong JS, Shin WJ, Lee YJ, Hong KO, Lee JI, Hong SP and Hong SD 2011 The role of Cripto-1 in the tumorigenesis and progression of oral squamous cell carcinoma. *Oral Oncol.* **47** 1023−1031

Corresponding editor: Sᴏʀᴀʙ Dᴀʟᴀʟ